Energy Conversion and Management 72 (2013) 156–162

Contents lists available at SciVerse ScienceDirect

Energy Conversion and Management

journal homepage: www.elsevier.com/locate/enconman

# Performance exploration of an energy harvester near the varying magnetic field of an operating induction motor

Yunus Uzun [a], Erol Kurt [b,*]

[a] Department of Electrics and Energy, Vocational School, Ahi Evran University, 40100 Kirsehir, Turkey
[b] Department of Electrical and Electronics Engineering, Faculty of Technology, Gazi University, 06500 Teknikokullar, Ankara, Turkey

ARTICLE INFO

*Article history:*
Available online 30 March 2013

*Keywords:*
Piezoelectric harvester
Magnetic field
Induction motor

ABSTRACT

This paper reports a performance exploration of a piezoelectric harvester which is positioned near an operating induction motor. The harvester includes a magnet knob in a pendulum arrangement, which ascertains mechanical vibrations under the varying magnetic field. This energy harvester transforms the ambient unused magnetic energy into the electricity due to the piezoelectric layer attached to the pendulum. It has been proven that when the motor is under operation, the varying ambient field causes a varying magnetic force at the tip of harvester, then output voltage between the terminals of piezoelectric layer is produced due to the mechanical vibrations. This output signal has some characteristics of the operating induction motor in terms of its operation frequency, number of magnetic pole and natural frequency of the harvester. Since the surrounding field of the induction motor directly depends on the current flowing through the windings and electrical parameters, both the amplitude $U$ and the frequency $\omega_m$ of the harvested voltage can be characterized after some certain parametrical explorations. It has been proven that the harvested voltage strictly depends on the electrical load, which is attached to the terminals of the harvester, after the rectifying circuit. The harvested power per surrounding volume can be increased up to 0.11 mW/cm$^3$, if the entire surrounding volume of the motor is considered.



## 1. Introduction

Energy harvesting from the ambient vibrations gets great interest for the improvement of the regenerative systems in autonomous sensor nodes and microsystems [1,2]. Presently, harvesters are used not only in the energy requirements of microsystems, but also in the macrosystems such as bicycles, railways and bridges [3–5]. Portable and wireless devices such as cell phones, MP3 players and navigators can also have efficient battery life by using different harvesting mechanisms. Among these mechanisms, the conversion of mechanical energy from ambient vibrations into electrical energy via a piezoelectric (PZT) converter is the most common way [1,6,7]. However, it is known that the effective harvesting process in such a converter becomes maximum, if the system operates in resonance frequency [8]. In reality, the energy obtained considerably decays in frequency-varying systems due to so-called wide-band vibrations. It is known that most of the ambient vibrations include harmonics. Therefore, the researchers consider to add other external strengths in order to achieve high harvesting efficiencies at complex vibrations [1,9,10]. One is magnetic field which yields to wide-band spectra of harvester displacement for increasing the output power at complex media. A recent study has proven that wide-band vibrations of the displacement increases the power of different harvester systems [1]. Ferrari and his colleagues [1] have proven that the wideband frequencies of displacement, which are resulted by the permanent magnets can improve the output power up to 250% in magnetically-excited piezoelectric layers. Within this context, as in our recent paper, the effect of magnetic excitation on such harvesters has also been explored in a pendulum-like harvester [8,11]. Although the strength of the field increases output power, the wide-band spectra of harvester velocity does not assist to get high powers. Therefore many different designs under various magnetic excitation types exist in the literature in order to clarify the dynamical and electrical features of the harvesters [1,9–12]. Among them, another harvester including four permanent magnets in a homogeneously exerted magnetic field can be mentioned, too [9]. Cottone et al. [9] explored some dynamical features of stochastically nonlinear vibrations and generated an energy output by using an external stable magnetic media. Since they used many permanent magnets and a stable magnetic field excitation, their system requires a large space for installation.

In the present paper, we motivate ourselves to explore the performance of alternative energy generation from the varying unused magnetic field of an induction motor while it is operating under a certain rotation rate. It will be shown that the power density of

* Corresponding author. Tel./fax: +90 3122028518.
*E-mail addresses:* yuzun@ahievran.edu.tr (Y. Uzun), ekurt@gazi.edu.tr (E. Kurt).

0196-8904/$ - see front matter © 2013 Elsevier Ltd. All rights reserved.
http://dx.doi.org/10.1016/j.enconman.2012.10.023

3 mW/m$^2$ can be harvested from the harvester system, when the entire surface of the motor is considered. The vibrations stem from the magnetic force are found to be sinusoidal and the harvester output voltage exhibits the behavior of magnetic force.

## 2. Energy harvesting setup

The setup for the energy harvester is sketched in Fig. 1a and the entire experimental system is shown in Fig. 1b. The setup mainly consists of five units: An operating induction motor, piezoelectric beam and permanent magnet attached to the piezoelectric thin layer (Lead zirconate titanate, i.e. PZT), laser displacement sensor (LDS), rectifier and storage circuit, and data acquisition and monitoring unit. The system arranged as a pendulum including a magnet knob (having 1 cm × 1 cm × 1 cm size) at the tip of the pendulum. The piezoelastic layer has been positioned at the top of the pendulum connecting the non-ferromagnetic beam to the clamp. The permanent magnet at the beam tip has the dimensions of 20 mm × 5 mm × 4 mm.

The varying magnetic force which is produced by the induction motor in operation affects the beam tip and an oscillation occurs at the harvester, thus a measurable voltage signal is generated at the output of PZT material. The oscillation is mainly characterized by the varying magnetic force which is interacted by the magnetic field of permanent magnet at the harvester tip. Since there exist elastic force and the damping effects in this energy system, we have focused on some nonlinear features of this system in some of our earlier studies, when a controlled electromagnet was used for the field excitations [8,11]. Due to the varying magnetic field of the motor with a certain synchronous speed $N_s$, the flux lines inside the stator core of the motor vary. Since the magnetic force is greater than the damping force, the harvester fluctuates with certain amplitude by elastic restoring forces. The laser displacement sensor (LDS) measures the displacement of the tip with a high accuracy during the operation and the tip velocity can also be determined by evaluating the position data at an exact time. The generated voltage signal can be controlled, stored and observed via a computer. Then, voltage generated by the piezoelastic harvester can be used to drive the load $R_L$ after it has been rectified.

The block diagram of the energy harvester is shown in Fig. 2. Because of the magnetic force, the piezoelectric layer generates voltage signals with certain harmonics. Then this signal is rectified by a full-wave rectifier shown in Fig. 3. The resulting voltage can be used to be stored in a capacitor or directly given to the load $R_L$. However, the load is vital to have the maximal power as will be shown in the next section. Therefore we use a variable resistive load in order to operate at the maximal power.

PZT layer with the sizes of 70 mm × 32 mm × 1.5 mm and the weight of 10 g was used in the experiments. The capacitance and stiffness values of PZT layer are 23.4 nF and 318 N/m, respectively. The laser displacement sensor (LDS) has a head with type *IL-065* and a control unit IL-1000 made by Keyence Inc. An NI USB-6250 data acquisition unit was also used in the setup. The induction motor has the dimensions of 16 cm in diameter and 20 cm in length, the power of 373 W, with delta connection, operating under 380 V and 50 Hz and having 4 poles. The laser displacement sensor measures the displacement of the beam tip and has a sensitivity of 4 μm. This laser displacement sensor head can measure the vibrations with the sampling rate of 1 ms. The data acquisition card has

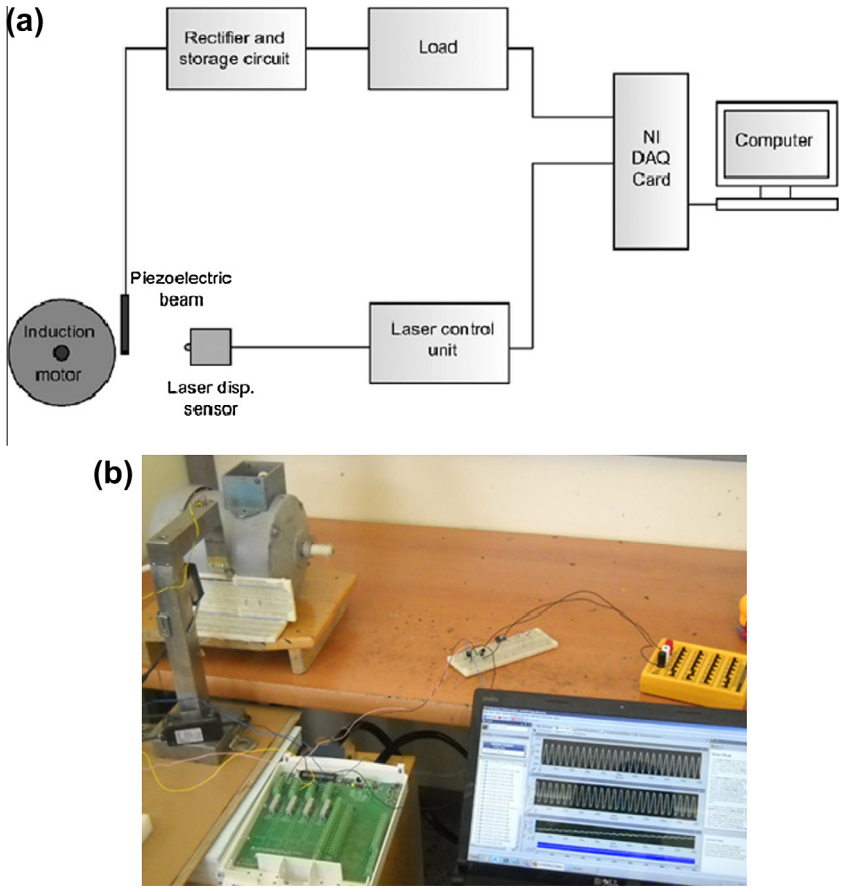


**Fig. 1.** (a) A sketch of energy harvester system near an operating induction motor. (b) The experimental setup with required units. Experimental setup: From left to right, laser displacement sensor (LDS), piezoelectric layer with permanent magnet, induction motor, DAQ card, rectifier circuit, variable resistive load and laptop.

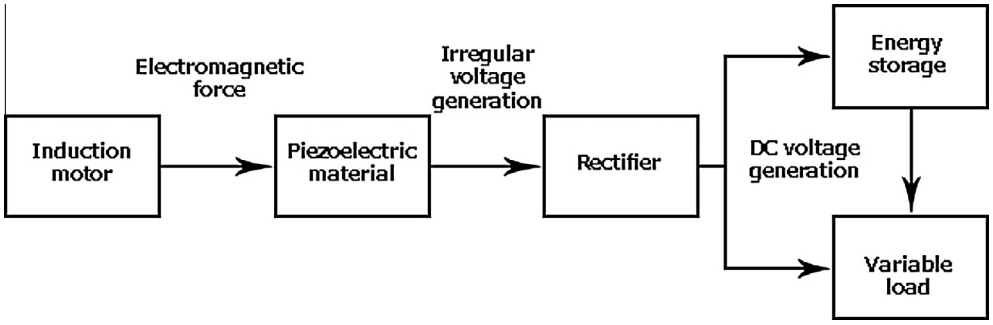


**Fig. 2.** Block diagram of the piezoelectric energy harvester.

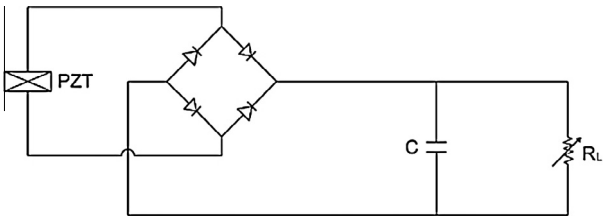


**Fig. 3.** The electrical circuit to get the harvested voltage and store in the capacitor. The diodes, capacitor and the load resistance minimal and maximal values are *1N4001*, 10 uF and $R_L$ = 10 kΩ to 10 MΩ.

16 analog inputs, thereby it is possible to get multiple records of different physical parameters such as displacement, output voltages from the PZT layer and rectifier/storage system, synchronously. For the data treatment and documentation, we collect all experimental outputs into the *LabView* software.

## 3. Theory of energy harvesting under varying magnetic ambient

In our earlier paper [13], some mechanical features of an elastic beam under a varying magnetic ambient were explored. However, the effect of the magnetic field on the energy-generation mechanism has not been investigated for a pendulum-like PZT harvester. A varying field near the harvester as seen in Fig. 1b can be modeled as an elastic beam with a permanent magnet attached to the tip of the beam (i.e. piezoelectric layer near an electromagnet). According to our previous studies [13,14], a varying field could be created near the tip of an electromagnet and this can drive the knob spatio-temporally and this model can give efficient results in order to compare theory with experiments.

Considering the varying magnetic force $F_m(x, i, t)$ exerted from the stator of the induction motor, a finite element method for a specific knob can achieve better theoretical results on the proposed energy system, when a sufficient number of mesh nodes in horizontal and vertical directions are used. In order to simplify the magnetic field effect on the harvester, the stator part is considered to be an electromagnet with a winding coil and a core. The force term was found by the fitted values of the simulation together with an electrical component indicating the temporal behavior of the modeled stator part. Thus the total magnetic force term $F_m$ can be considered as a polynomial expression after the position scaling:

$$F_m(t) = \{(1 - 0.7056/d) + 0.0623(1-u) + 28026d(1-u)^2 - 10^6\, d^2(1-u)^3\}\,\{8\times10^{-8} i_c(t)^2 - 10^{-9} i_c(t)\}$$

$$i_c(t) = \begin{cases} \frac{V_c}{R_c}(1 - e^{-R_c t/L}) & 0 < t \leqslant \frac{T}{2} \\ \frac{V_c}{R_c} e^{-R_c t/L} & \frac{T}{2} < t \leqslant T \end{cases} \quad (1)$$

Here $u$, $d$, $V_c$, $R_c$, $L$ denote the mass displacement, the distance from the stator to the pendulum equilibrium, voltage, resistance and inductance of stator coil, respectively. For the simplicity, we consider a purely resistive load directly connected to PZT as in many other studies [15–17]. The quantities in Eq. (1) define the electrical features of this electromagnet. Such a finite element analysis clarifies a magnetostatic solution at first, whereas the resulting magnetic force values can be generalized as functions of time and winding current inside the coil as will be shown later. Table 1 gives the parameters, which are stated in Eq. (1) and used in the experiments.

By the inclusion of varying field to the model, the harvester model should include the mechanical and electrical aspects as in Fig. 4. Strictly speaking, the entire system can be modeled as a mass-spring, a damper and a capacitor. Here the rigid mass $m_p$ and the stiffness constant $k$ determine the mechanical structure under a damper $\gamma$ which gives the mechanical losses.

If a mass displacement $u$ occurs inside the piezoelectric material, an electrical current $i$ and a voltage $V$ are generated. Therefore a relation between the mechanical and electrical units can be written as,

$$F_{total} = ku + \alpha V + F_m,$$

$$i = \alpha \frac{du}{dt} - C\frac{dV}{dt}. \quad (2)$$

where $C$ is the clamped capacitance and $\alpha$ is the force factor. The total dynamic equation of the harvester can be written as follows:

$$\frac{d^2x_i}{dt_i^2} = \left(-\gamma\frac{du_i}{dt_i} - m_p\frac{d^2u_i}{dt_i^2} - ku_i - \alpha V - F_m(t)\right)\frac{1}{(m+m_p)}. \quad (3)$$

Here $u_i(t)$ and $x_i(t)$ indicates the mass displacement inside PZT and the pendulum displacement, respectively, whereas $m$ denotes the total mass with magnet and PZT. By considering the varying field $F_m$, the overall dynamics and electrical equations can be stated as follows:

$$\frac{d^2x_i}{dt_i^2} = -\frac{\gamma}{(m+m_p)}\frac{du_i}{dt_i} - \frac{1}{(\frac{m}{m_p}+1)}\frac{d^2u_i}{dt_i^2} - \frac{k}{(m+m_p)}u_i - \frac{\alpha}{(m+m_p)}V - \frac{1}{(m+m_p)}F_m(t),$$

**Table 1**
Experimental parameters.

| | |
|---|---|
| $d$ | Between 2.7 and 3.3 mm |
| $V_c$ | 380 V |
| $R_c$ | 20.3 Ω |
| $L$ | 158 mH |

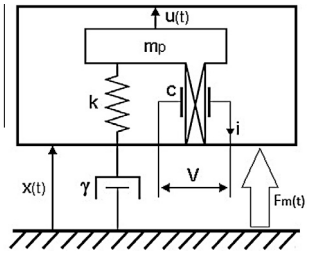


**Fig. 4.** Energy harvester model of a piezoelectric beam under magnetic excitation $F_m(t)$.

$$\frac{dV_i}{dt_i}=\frac{\alpha}{C}\frac{du_i}{dt_i}-\frac{i}{C}. \tag{4}$$

Above $F_m$ indicates the periodically changing magnetic force referred in Eq. (1). Here the mechanical losses are shown proportional to the velocity of the pendulum as in many other studies [1,8,12]. Since the amplitude $x$ is directly proportional to the displacement $u$, one reads as $u_i = x_i$. Thus, the resulting equation can be simplified as,

$$\frac{d^2u_i}{dt_i^2}=-\frac{\gamma}{m+2m_p}\frac{du_i}{dt_i}-\frac{k}{m+2m_p}u_i-\frac{\alpha}{m+2m_p}V-\frac{1}{m+2m_p}F_m(t),$$

Thus, the first equation of Eq. (4) yields to

$$V=\frac{uR_L\alpha jN_s\{(m+m_p)N_s^2-F_0\langle I_c^2\rangle+F_1\langle I_c\rangle\}}{(-\gamma jN_s-m_pN_s^2-k)(1+R_LCjN_s)-\alpha^2R_LjN_s}+\text{higher order terms}, \tag{8}$$

after an arithmetic manipulation, since the harvester is driven by the synchronous speed $N_s$ (i.e. 25 Hz). The linear terms of the piezoelectric amplitude $u$ are considered in order to have an expression on generating power by using the above equations. Above $\langle I_c\rangle$ and $\langle I_c^2\rangle$ denote the time-averaged values of Eq. (1) as indicated below:

$$\langle I_c\rangle=\frac{V_c}{2R_c}+\frac{V_cL\omega_m}{2\pi R_c^2}\left(2e^{-\frac{R_c\pi}{L\omega_m}}-1-e^{-\frac{R_c2\pi}{L\omega_m}}\right),$$

$$\langle I_c^2\rangle=\frac{V_c^2}{2R_c^2}+\frac{V_c^2L\omega_m}{4\pi R_c^3}\left(1-e^{-\frac{R_c4\pi}{L\omega_m}}\right)+\frac{L\omega_m}{\pi R_c}\left(e^{-\frac{R_c\pi}{L\omega_m}}-1\right), \tag{9}$$

after the time integration during a certain period. Note that the electrical parameters above belong to the coil while a certain voltage $V_c$ with a frequency of $\omega_m = 2\pi f$ ($f = 50$ Hz) is applied to the windings of the stator. In that case, one can arrive at the power relation as follows:

$$\langle P\rangle=\frac{u^2R_L\alpha^2N_s^2\{(m+m_p)N_s^2-F_0\langle I_c^2\rangle+F_1<I_c>\}^2}{k^2(1+C^2R_L^2N_s^2)+2kN_s^2(m_p+\alpha^2CR_L^2+C^2m_pR_L^2N_s^2)+N_s^2\{2\alpha^2\gamma R_L+\alpha^4R_L^2+2\alpha^2Cm_pR_L^2N_s^2+\gamma^2(1+C^2R_L^2N_s^2)+m_p^2N_s^2(1+C^2R_L^2N_s^2)\}} \tag{10}$$

$$\frac{dV_i}{dt_i}=\frac{\alpha}{C}\frac{du_i}{dt_i}-\frac{i}{C}. \tag{5}$$

Eq. (5) can then be used for the overall determination of the system in mechanical and electrical manner.

For the dimensionless form of Eq. (5), $t_i = \tau t$, $y_i = yd/\tau$, $u_i = ud$ and $V_i = V_0V$ are introduced for time, velocity, position and voltage scaling, respectively. $\tau$ determines the natural period of the pendulum and cannot be confused by the excitation period of the magnetic field $T$. To avoid the misunderstanding, $d$ in later two expressions refers to the distance between the equilibrium point of harvester and the stator core. Then the dimensionless form can be stated as follows:

$$\frac{du}{dt}=y,$$

$$\frac{dy}{dt}=-\frac{\gamma\tau}{m+2m_p}y-\frac{k\tau^2}{m+2m_p}u-\frac{(m+m_p)\tau^2F_m(t)}{(m+2m_p)d}-V\times\frac{\alpha\tau^2V_0}{(m+2m_p)d},$$

$$\frac{dV}{dt}=\frac{\alpha d}{CV_0}\frac{du}{dt}-\frac{\tau V}{V_0CR_L}. \tag{6}$$

The position difference $d$ transfers the coordinate system into the equilibrium point since the amplitude of the pendulum is represented by $u$. To find out the averaged power output as a theoretical assumption, Eq. (4) is considered in frequency domain. While the second equation in Eq. (4) is written as,

$$V=\frac{jR_L\alpha N_su}{1+jCR_LN_s}, \tag{7}$$

From the linear part of Eq. (8) w.r.t. $u$ and its complex conjugate divided by load resistance $R_L$ (i.e. $\langle P\rangle = \langle VV^*\rangle/R_L$), Eq. (10) gives a complete relation between the output harvester power and both the electrical and mechanical parameters of the system. By using Eq. (10), it is also possible to find out the optimal load resistance, analytically. If the derivative of this equation w.r.t $R_L$ is taken, the optimal load resistance can also be estimated as $(N_s\,C)^{-1}$ (for a detailed approximation in the case of different system, see [3]). Here $N_s$ gives the synchronous frequency of magnetic flux steaming

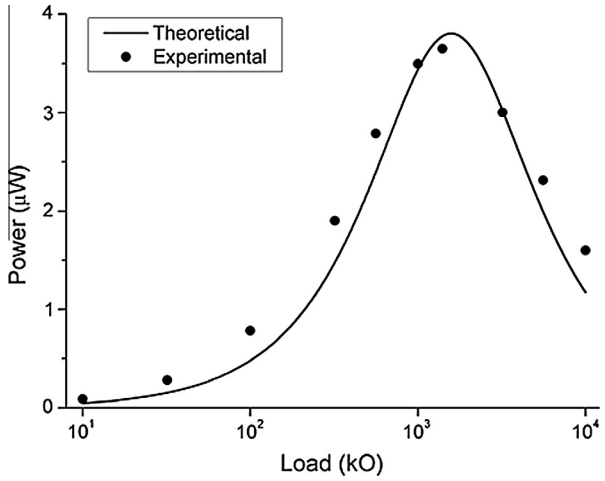


**Fig. 5.** The comparison of experimental (from Fig. 8) and theoretical output powers as functions of load resistance $R_L$. The distance $d$ from the equilibrium point to the motor is 0.3 cm and the voltage over the stator winding is 380 V throughout the experiment.

from coils and $C$ is the capacitance of the piezoelectric layer, respectively.

To prove the consistence of the theoretical model with the experimental data obtained from the experimental system in Fig. 1, a comparison between the power generations from theoretical model and experimental study is shown in Fig. 5. Here the load resistance $R_L$ connected to the output of the piezoelectric layer plays an important role to obtain the maximal power from the system. The theoretical results in the plot have been obtained from Eq. (10). In this equation, the amplitude of piezoelectric layer $u = 0.3$ mm, the force/voltage ratio $\alpha = 0.0001$ N/V, $N_s = 25$ Hz, total mass $m = 15$ g, piezoelectric layer mass $m_p = 10$ g, magnetic force coefficients $F_0 = 5000$, and $F_1 = 7200$, elastic stiffness coefficient $k = 318$ N/m, piezoelectric layer capacitance $C = 23.4$ nF, damping ratio $\gamma = 10.44$, inductance of winding $L = 158$ mH and resistance of winding $R_c = 20.3\ \Omega$ are used, respectively. Fig. 5 proves that the optimal power is obtained for a specific load resistance about $R_L = 1.5\ \mathrm{M}\Omega$ in both theory and experiment. The detailed observations have shown that above and below of this load, the output power substantially decreases.

## 4. Results and discussion

In this section, the experimental results on the harvested electrical energy from the induction motor are discussed. We refer to one of our previous study [8] for some preliminary studies on the nonlinear responses under a varying field generated by an electromagnet in terms of different excitation frequencies. It has been found that the main energy producing mechanism is strictly related to the displacement of the PZT layer from the equilibrium point in such a system. In Fig. 6a and b, we present some representative generated voltage plots. Since the harvester tip oscillates regularly with respect to the time-variance of the magnetic flux inside the induction motor, we have a sinusoidal harvested voltage. The voltage is not fully sinusoidal, since the negative alternance of the generated voltage is taken to the positive side. Without capacitance, the negative part of the signal is destroyed and the signal has certain ripples at the minimal points due to the voltage drops in diodes. In addition, this harvested signal can be transformed into a direct current if an appropriate capacitor is used after the rectifier as seen in Fig. 6b. A corresponding FFT of the gen-

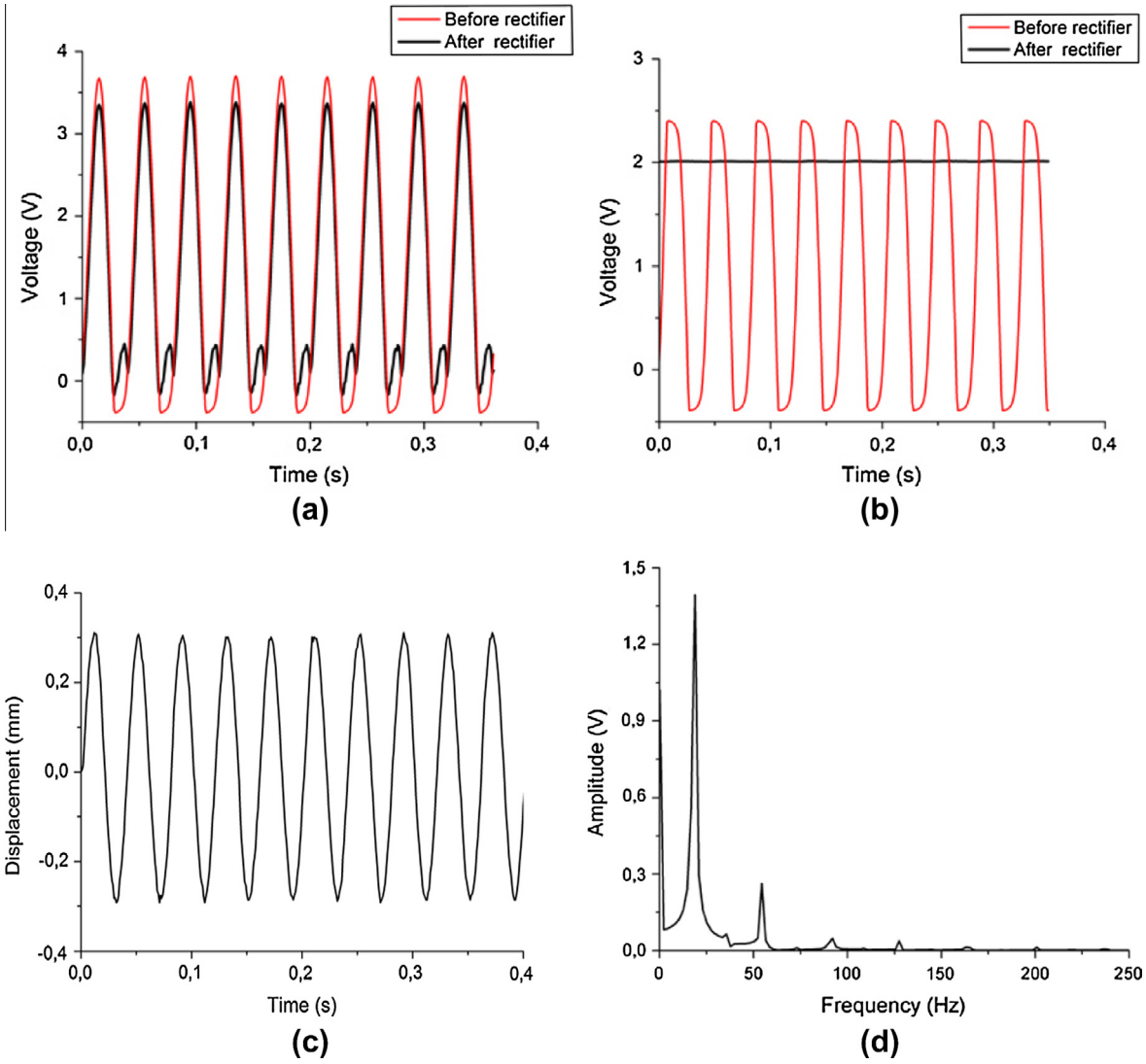


**Fig. 6.** (a) The generated voltage before and after the rectifier unit at the lack of the capacitor and (b) with capacitor. (c) The displacement of harvester tip as function of time. (d) The FFT of the generated voltage signal in (b) before the rectifier, when the capacitor exists.

erated voltage just after the harvester output is shown at Fig. 6d. According to FFT, the main frequency is found to be $f = 18$ Hz. This frequency is the nonlinear combination of the natural oscillation frequency of the harvester (i.e. $f_0 = 23.2$ Hz) and the synchronous speed of the induction motor $N_s = 25$ Hz). One clarifies that the synchronous speed of the motor, $N_s = 25$ Hz can be found by the flux varying frequency of 4 poled motor as given in the formulation of [18]:

$$N_s = \frac{120f}{p} \tag{11}$$

Here $N_s$ is synchronous speed, $f$ is supply frequency and $p$ is number of poles for which the stator winding is positioned and $p$ cannot be confused with power in the (Eq. (10)). According to the above formulation, $N_s$ is found to be 1500 rpm and it is converted to 25 Hz, which is close to the main frequency in FFT of voltage. According to our unpublished studies, the excitation frequency of the field cannot drive the harvester with the excited frequency, since the amplitude of the magnetic force is small. Therefore the effect of the natural frequency $f_0$ increases in order to change the frequency of the generated voltage from the synchronous speed value $N_s = 25$ - Hz. Note that there also exist certain higher harmonics (i.e. 36 Hz, 54 Hz, 90 Hz and 126 Hz) in the harvested signal just after the PZT layer. Therefore an efficient rectifying mechanism is required in order to harvest a regular electrical energy from this system.

According to one of the previous studies, the frequency of the magnetic force causes certain harmonics in the tip velocity in such systems [8]. In fact, when the frequency of the magnetic force becomes different from the natural frequency of the system, there exists a number of harmonics in the velocity data. The nonlinear character in the output signal increases, when the magnetic force decreases. However the harmonicity in velocity data does not affect the generated voltage in the earlier experiments. In addition, we consider that the flux inhomogeneties can also produce higher harmonics in such a system. Fig. 6c represents the periodic displacement of the harvester tip around the equilibrium point. Although the displacement is periodic, the harvester voltage is skipped to positive part in Fig. 6a and b, when the rectifier unit is attached to the harvester.

At the left hand-side of Fig. 7, the stored electrical energy is plotted as function of time in terms of different resistive loads. This plot proves that a certain resistance value is needed in order to harvest the optimum energy from such a system due to the fact that the material structure of the PZT layer includes capacitive and resistive features. The right graph shows the stored energy in capacitor without any electrical load. According to our results, nearly 0.18 mJ energy can be stored in the harvester capacitor in 100 s. This energy amount is obtained from only one PZT layer with the dimensions of 70 mm × 32 mm × 1.5 mm. In order to have a much comprehensive idea on the energy generation, we have plotted the harvested power in Fig. 8.

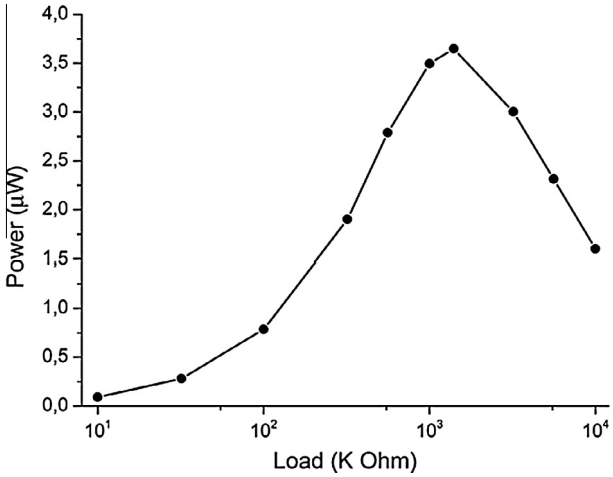


**Fig. 8.** Experimental generated power as function of resistive loads.

When the resistive load is adjusted about $R_L = 1.5$ MΩ, a certain maxima in power is obtained. This maximal value is observed to be $P = 3.8$ μW. According to our experiments, the power density of the PZT layer $P_S = 1.13$ μW/cm$^3$ can be available, if a unit volume of PZT is considered. However, if the total surrounding area of the motor is considered to be covered by this PZT layer, the amount of 0.11 mW/cm$^3$ power can be available from such a small induction motor, when nearly 100 PZT layer is wrapped on the motor surface.

## 5. Conclusions

The feasibility of harvesting mechanism on an operating induction motor has been explored experimentally and analytically. The motor operates without any mechanical load. The harvester is designed and manufactured in a pendulum type with a magnet knob, which can be affected by a variable magnetic field occurred by the motor surroundings. It has been observed that the resistive load at-

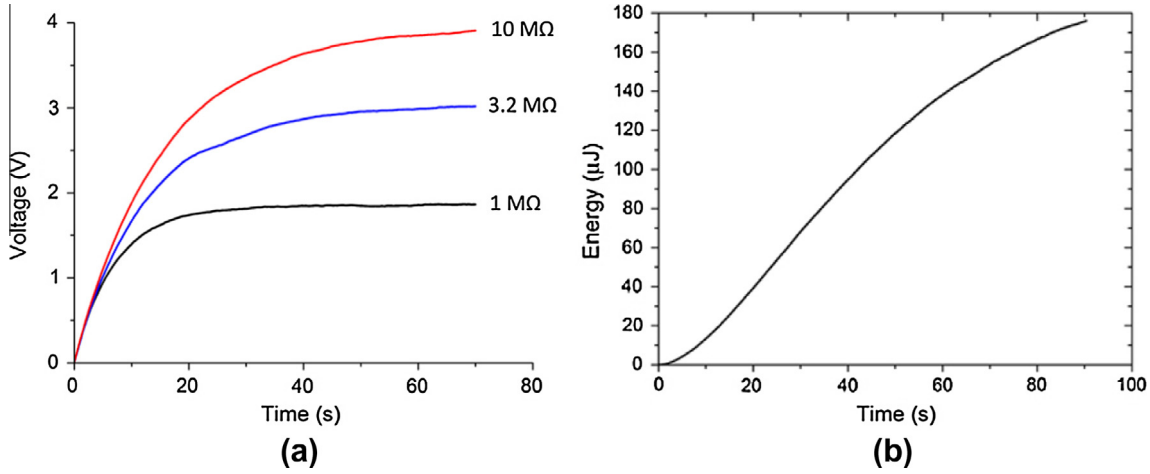


**Fig. 7.** (a) Harvested voltages as function of time after the rectifier circuit in the cases of different resistive loads. (b) Electrical energy stored in the capacitor as function of time.

tached at the output of the rectifier plays an important role to harvest the maximal power from this system. The output signal includes a number of harmonics. The experiments prove that at least 0.11 mW/cm$^3$ power per surrounding volume can be available from this harvester. In fact, the effects of magnetic flux outside the motor can be increased further, when the motor operates under a mechanical load. The current flowing in the stator should be increased for a certain amount, if it is on the mechanical load. Thus the system can be used as an alternative energy source converting the magneto-mechanical energy into the electrical energy in factories, dams, etc. Since electromagnetic and electrostatic systems are alternative to the magneto-piezoelectric systems, one can make a comparison on those systems. It has been known that energy density of piezoelectric systems under magnetic media can lead to higher energy densities compared to the ones consisting of pure electromagnetic or electrostatic systems and piezoelectric systems can generate higher voltages up to 10 V compared to the electromagnetic energy converting systems. Therefore it can be stated that the piezoelectric harvesters are much promising, when they are configured as a compact system on the surrounding area of magnetic devices.

## Acknowledgements

The authors acknowledge the support of Gazi University – Scientific Research Project Unit under the Project No: BAP 07/2010-01 and EU ERASMUS Intensive Programme EWRES 2012, which took place in Antalya/Turkey between 17–28 Sep. 2012.

## References

[1] Ferrari M, Ferrari V, Guizzettia M, Andò B, Baglio S, Trigona C. Improved energy harvesting from wideband vibrations by nonlinear piezoelectric converters. Sensor Actuat A 2010;162:425–31.
[2] Cook-Chennault KA, Thambi N, Sastry AM. Powering MEMS portable devices-a review of non-regenerative and regenerative power supply systems with special emphasis on piezoelectric energy harvesting systems. Smart Mater Struct 2008;17:1–33.
[3] Minazara E, Vasic D, Costa F. Piezoelectric generator harvesting bike vibrations energy to supply portable devices. In: International conference on renewable energies and power quality, Spain; 2008.
[4] Kong N, Ha DS, Erturk A, Inman DJ. Resistive impedance matching circuit for piezoelectric energy harvesting. J Intel Mater Syst Struct 2010;21:1293–302.
[5] Dayou J, Man-Sang C. Performance study of piezoelectric energy harvesting to flash a LED. Int J Renew Energy Res 2011;1(4):323–32.
[6] Mitcheson PD, Yeatman EM, Rao GK, Holmes AS, Green TC. Energy harvesting from human and machine motion for wireless electronic devices. Proc IEEE 2008;96:1454–86.
[7] James EP, Tudor MJ, Beeby SP, Harris NR, Glynne-Jones P, Ross JN, et al. An investigation of self-powered systems for condition monitoring applications. Sens. Actuators A 2004;110:171–6.
[8] Uzun Y, Kurt E. Implementation and modeling of a piezoelastic pendulum under a harmonic magnetic excitation. In: 11 International conference applications of electrical engineering, Greece; 2012.
[9] Cottone F, Vocca H, Gammaitoni L. Nonlinear energy harvesting. Phys Rev Lett 2009;102:080601.
[10] Zhu D, Tudor MJ, Beeby SP. Strategies for increasing the operating frequency range of vibration energy harvesters: a review. Meas Sci Technol 2010;21:1–29.
[11] Uzun Y, Kurt E. Energy harvesting from the varying magnetic field of an operating induction motor. In: IIIrd International conference on nuclear and renewable energy resources, Turkey; 2012.
[12] Stanton SC, McGehee CC, Mann BP. Nonlinear dynamics for broadband energy harvesting: investigation of a bistable piezoelectric inertial generator. Phys D 2010;239:640–53.
[13] Kurt E. Nonlinear responses of a magnetoelastic beam in a step-pulsed magnetic field. Nonlinear Dyn 2006;45:171–82.
[14] Kurt E, Kasap R, Acar S. Effects of periodic magnetic field to the dynamics of vibrating beam. Math Comp Appl J 2004;9:275–84.
[15] Challa VR, Prasad MG, Fisher FT. A coupled piezoelectric–electromagnetic energy harvesting technique for achieving increased power output through damping matching. Smart Mater Struct 2009;18:095029.
[16] Ottman GK, Hofmann HF, Bhatt AC, Lesieutre GA. Adaptive piezoelectric energy harvesting circuit for wireless remote power supply. IEEE Trans Power Elect 2002;17:669–76.
[17] Cho JH, Richards RF, Bahr DF, Richardsa CD. Efficiency of energy conversion by piezoelectrics. Appl Phys Lett 2006;89:104107.
[18] Bakshi UA, Godse AP. Electrical machines & electronics. 1st ed. India: Technical Publications; 2009.